Chemosphere 221 (2019) 452–463

Contents lists available at ScienceDirect

Chemosphere

journal homepage: www.elsevier.com/locate/chemosphere

Investigating the $PM_{2.5}$ mass concentration growth processes during 2013–2016 in Beijing and Shanghai

Jinjin Sun [a], Mingjie Liang [a], Zhihao Shi [a], Fuzhen Shen [a], Jingyi Li [a], Lin Huang [a], Xinlei Ge [a], Qi Chen [b], Yele Sun [c], Yanlin Zhang [d], Yunhua Chang [d], Dongsheng Ji [c], Qi Ying [e], Hongliang Zhang [f], Sri Harsha Kota [g], Jianlin Hu [a, *]

[a] Jiangsu Key Laboratory of Atmospheric Environment Monitoring and Pollution Control, Collaborative Innovation Center of Atmospheric Environment and Equipment Technology, Nanjing University of Information Science & Technology, Nanjing 210044, China
[b] State Key Joint Laboratory of Environmental Simulation and Pollution Control, College of Environmental Sciences and Engineering, Peking University, Beijing 100871, China
[c] State Key Laboratory of Atmospheric Boundary Layer Physics and Atmospheric Chemistry, Institute of Atmospheric Physics, Chinese Academy of Sciences, Beijing 100029, China
[d] Yale-NUIST Center on Atmospheric Environment, Nanjing University of Information Science & Technology, Nanjing 210044, China
[e] Zachry Department of Civil Engineering, Texas A&M University, College Station, TX 77843-3136, USA
[f] Department of Civil and Environment Engineering, Louisiana State University, Baton Rouge, LA 77803, USA
[g] Department of Civil Engineering, Indian Institute of Technology Delhi, New Delhi 110016, India

HIGHLIGHTS

- $PM_{2.5}$ growth processes during 2013–2016 in the NCP and YRD region of China were investigated.
- 4-year averaged PMRRs of $PM_{2.5}$ total mass are $7.07 \pm 8.42\ \mu g\ m^{-3}\ h^{-1}$ in BJ and $6.60 \pm 5.99\ \mu g\ m^{-3}\ h^{-1}$ in SH.
- Organic aerosol is more important in BJ, while nitrate is more important in SH.
- The PM2.5 growth processes in BJ and SH are proposed to be classified into four general categories.

ARTICLE INFO

Article history:
Received 18 September 2018
Received in revised form
27 December 2018
Accepted 30 December 2018
Available online 4 January 2019

Handling Editor: R Ebinghaus

Keywords:
Beijing
Shanghai
$PM_{2.5}$
Growth processes
Chemical composition
Sources

ABSTRACT

The North China Plain and the Yangtze River Delta are the two of the most heavily polluted regions in China. Observational studies revealed that 'explosive' $PM_{2.5}$ mass concentration growths frequently occurred in the two regions. This study analyzed all the $PM_{2.5}$ mass concentration growth processes from clean condition (i.e., $<35\ \mu g\ m^{-3}$) to heavy pollution condition (i.e., $>150\ \mu g\ m^{-3}$) in Beijing (BJ) and Shanghai (SH), two representative cities of the two regions, using hourly monitored $PM_{2.5}$ concentrations during 2013–2016. 173 and 76 growth processes were identified in BJ and SH, respectively. $PM_{2.5}$ rising rates (PMRR) and dynamic growth durations were calculated to illustrate the characteristics of the growth processes. Hourly particulate chemical composition data and meteorological data in BJ and SH were further analyzed. The 4-year averaged PMRR of $PM_{2.5}$ total mass were similarly of $7.11 \pm 9.82\ \mu g\ m^{-3}\ h^{-1}$ in BJ and $6.71 \pm 6.89\ \mu g\ m^{-3}\ h^{-1}$ in SH. A decreasing trend was found for the $PM_{2.5}$ growth processes in two cities from 2013 to 2016, reflecting the effectiveness of emission controls implemented in the past years. The contributions of particulate components to the $PM_{2.5}$ total mass growth were different in BJ and SH. Average PMRR value of PM_1 organic aerosols (OA), SO_4^{2-}, NO_3^-, and NH_4^+ in BJ was 1.90, 0.95, 0.82, and $0.53\ \mu g\ m^{-3}\ h^{-1}$, respectively. Average PMRR of $PM_{2.5}$ OA, SO_4^{2-}, NO_3^-, and NH_4^+ in SH was 1.70, 1.18, 1.99 and $1.14\ \mu g\ m^{-3}\ h^{-1}$, respectively. Based on the contributions of different components, the $PM_{2.5}$ mass concentration growth processes in BJ and SH were proposed to be classified into 'other components-dominant growth processes', 'all components-contributing growth processes', 'one or more explosive secondary components-dominant growth processes', and 'mixed-factor growth processes'. Potential source contribution function analysis and the meteorological condition analysis showed that source origins and prevailing wind for the two cities during different categories of growth processes had substantial difference. The important source areas included Hebei and Shandong for BJ, and Jiangsu and

* Corresponding author.
E-mail address: jianlinhu@nuist.edu.cn (J. Hu).

https://doi.org/10.1016/j.chemosphere.2018.12.200

Anhui for SH. The dominant wind directions during growth processes were northeast, south and southwest in BJ, and were west to north in SH. The results suggested the contributing components, the prevailing wind conditions, and the formation processes were substantially different in the two cities, despite the similar PMRR of $PM_{2.5}$ total mass during the growth processes between BJ and SH. Future research is needed to study the detailed formation mechanisms of the different $PM_{2.5}$ mass concentration growth processes in the two cities.

1. Introduction

China has been suffering from serious haze pollution characterized by high fine particulate matter ($PM_{2.5}$) concentrations in recent years, due to a large amount of air pollutant emissions with the rapid growth of energy consumption associated with the fast economic development and intensified urbanization (Bai et al., 2014). Especially, the North China Plain (NCP) and the Yangtze River Delta (YRD) are two of the regions with the most serious $PM_{2.5}$ pollution (Wang et al., 2015a; Zhang and Cao, 2015), and also they are the most populous and economically developed regions in China. Heavy $PM_{2.5}$ pollution is found to pose great threats to public health (Hu et al., 2017; Lelieveld et al., 2015; Liu et al., 2016a).

Studies have reported that $PM_{2.5}$ concentration could grow quickly in the two regions (Ji et al., 2014; Li et al., 2016; Lv et al., 2017; Sun et al., 2014). For example, Zheng et al. (2015) found that sharp increase in $PM_{2.5}$ concentrations could be up to several hundred $\mu g\ m^{-3}$ per hour recorded in Beijing (BJ), the capital city of China located in the NCP region, in January of 2012 and 2013. Sun et al. (2014) also observed that the PM_1 (i.e., particulate matter with aerodynamic diameters $< 1\ \mu m$) mass concentrations in BJ during January 12-13, 2013 were more than 10 times higher than those measured during clean periods. Li et al. (2016) found that the average $PM_{2.5}$ concentrations were 3.4 times higher during haze-fog than clean periods in Nanjing, a megacity located in the YRD region, in December 2013.

Many studies have been conducted in recent years to investigate the formation mechanisms of heavy haze air pollution in the two regions (Guo et al., 2014; Huang et al., 2014a; Sun et al., 2014, 2016; Wang et al., 2015a; Yang et al., 2015; Zheng et al., 2015). Several factors affecting $PM_{2.5}$ growth have been identified, including high primary emissions (Yang et al., 2016; Zhang et al., 2012b), regional transport from highly polluted areas (Chen and Xiang-De, 2017; Fu et al., 2016; Sun et al., 2017; Wu et al., 2017; Xue et al., 2014), secondary transformation (Quan et al., 2015; Tian et al., 2015; Wang et al., 2014b), as well as adverse and stagnant meteorological conditions (Fu and Chen, 2016; Wang et al., 2018b; Zhang et al., 2014b, 2015). For example, Kang et al. (2014) found that secondary compounds accounted for 49.8% of the total $PM_{2.5}$ in BJ during the winter of 2012. Huang et al. (2014b) found that secondary aerosol formation contributed 51% of $PM_{2.5}$ in episodes of severe haze pollution in BJ during January 2013. At an urban-industrial area of Nanjing in January of 2015, Yu et al. (2018) observed that the average mass concentration of the dominant water-soluble ions (SO_4^{2-}, NO_3^-, and NH_4^+) in $PM_{2.5}$ was about 2–3 times higher during the polluted periods than measured during the clean periods. In the other hand, Zhang et al. (2014b) found that more than 2/3 of the variance of observed evolution of the fog and haze event could be explained by the meteorological conditions (the weakened surface winds and the anomalous inversion in the near surface) over eastern China in January 2013.

Air pollution has become a top concern of the Chinese public, especially in the NCP and YRD regions (Chang et al., 2017, 2018; Huang et al., 2014b; Shu et al., 2017; Wang et al., 2015b; Zhang et al., 2014a, 2014b). Comprehensive pollution control strategies have been implemented, such as the Action Plan for Air Pollution Prevention and Control (2013) (Liang et al., 2017; Qiu, 2014), to improve air quality by reducing emissions of pollutants (mainly primary PM, SO_2, and NO_x) (Huang et al., 2013; Wang and Hao, 2012; Zhang et al., 2012a). As a result, annual average $PM_{2.5}$ concentrations have been declining since 2013 in the two regions (Wang et al., 2017b). However, severe haze pollution events in the two regions still occurred frequently during the past few years. It is urgent to understand the formation mechanism for the severe haze pollution events. Even though factors for individual events or processes have been identified in previous studies, the overall relative importance of the factors still remains unclear (Hu et al., 2015b; Sun et al., 2014; Yang et al., 2015). The objective of this study is to investigate the relative importance of controlling factors for different $PM_{2.5}$ mass concentration growth processes in the NCP and YRD regions. The results will improve our understanding of the mechanism of severe haze pollution events and help in designing effective strategies to improve air quality in the NCP and the YRD regions.

2. Data and methods

2.1. Study cities and data collection

In this study, we analyzed the dynamic accumulation of $PM_{2.5}$ using hourly concentrations between 18 January 2013 and 31 December 2016 in BJ and Shanghai (SH). BJ and SH is the biggest mega-cities in the NCP and YRD region, respectively (locations shown in Fig. S1 in the Supplemental Materials). Many studies have chosen BJ and SH to represent the air quality in NCP and YRD, such as (Hua et al., 2015; Ji et al., 2014; Yang et al., 2015). Hourly concentrations of $PM_{2.5}$ in BJ and SH from 18 January 2013 to 31 December 2016 were obtained from the publishing website of China National Environmental Monitoring Center (http://113.108.142.147:20035/emcpublish/). The measurement method for this dataset can be found in previous studies and the references therein (Hu et al., 2014, 2015a; Wang et al., 2014a).

Hourly PM_1 chemical composition of OA, SO_4^{2-}, NO_3^- and NH_4^+ in BJ was measured by an Aerodyne Aerosol Chemical Speciation Monitor from 1 January to 24 May 2013. The measurements were taken at Institute of Atmospheric Physics (IAP), Chinese Academy of Sciences (39°58′28″N, 116°22′16″E), which is located between the north 3rd and 4th ring road in BJ. The sampling site is located in the urban center, where most of the $PM_{2.5}$ mass monitoring sites are located. According to a study examining the spatial and temporal variations of criteria air pollutants in BJ using 1-year ambient monitoring data (Guo et al., 2017), the $PM_{2.5}$ among urban sites in Beijing is highly homogeneous. The descriptions of ACSM measurements and data analysis is given in Sun et al. (2012). Hourly $PM_{2.5}$ chemical composition of OC, SO_4^{2-}, NO_3^- and NH_4^+ in SH was measured by the Monitors for AeRosols and Gases (MARGA,

Applikon B.V., NL) (Chang et al., 2016) during 1 June 2014 to 31 December 2015. A ratio of 2 was used to convert OC to OA (i.e., OA = 2OC) (Xing et al., 2013; Zhang et al., 2014a).

2.2. $PM_{2.5}$ mass concentration growth processes

We focused on the $PM_{2.5}$ mass concentration growth processes from clean condition ($[PM_{2.5}]_{min}$) to heavy pollution condition ($[PM_{2.5}]_{max}$). $[PM_{2.5}]_{min}$ is the lowest $PM_{2.5}$ concentrations less than 35 $\mu g\,m^{-3}$ and $[PM_{2.5}]_{max}$ is the highest $PM_{2.5}$ concentrations greater than 150 $\mu g\,m^{-3}$. Examples of the $PM_{2.5}$ growth processes are presented in Fig S2. $PM_{2.5}$ concentration rising rates (PMRR) were defined in Eq. (1):

$$\mathrm{PMRR}\left(\mu g\cdot m^{-3}\cdot h^{-1}\right) = \frac{([\mathrm{PM2.5}]\ \max - [\mathrm{PM2.5}]\ \min)}{\mathrm{Duration\ (hour)}} \quad (1)$$

PMRR was used to illustrate the strength of the $PM_{2.5}$ mass concentration growth processes (Lv et al., 2017; Yang et al., 2015). In this study, PMRR and dynamic growth duration are calculated to illustrate the characteristics of the growth processes. All growth processes of $PM_{2.5}$ in BJ and SH during the four-year studying period were screened and PMRR of each growth process was calculated. In addition, identified $PM_{2.5}$ mass concentration growth processes during the periods with available composition measurements in BJ and SH were selected for further analyses. In total, 22 $PM_{2.5}$ mass concentration growth processes were identified in BJ and 19 processes were identified in SH with available composition measurement data. PMRR of each component was then calculated for these growth processes. Magnification of each chemical composition and $PM_{2.5}$ total mass were calculated by dividing the concentration at the end hour of the growth processes by the concentration at the beginning hour of the 41 $PM_{2.5}$ mass concentration growth processes. Then the magnification ratios (MR) were determined using the following equation:

$$\mathrm{MR} = \frac{\mathrm{Magnification\ of\ chemical\ \ composition}}{\mathrm{Magnification\ \ of\ PM2.5\ total\ mass}} \quad (2)$$

2.3. Meteorological and potential source contribution function (PSCF) analysis

Meteorological conditions during each growing process in BJ and SH were investigated, in order to further analyze the influence of meteorological factors on the $PM_{2.5}$ mass concentration growth processes. Meteorological parameters including wind speed (WS, m/s), wind direction (WD, °N), temperature (T, °C) and relative humidity (RH, %) were considered in this study. Meteorological observational data were obtained from the publishing website of National meteorological information center of China (http://data.cma.cn/data/). Meteorological characteristics for growing processes with different PMRR intervals were analyzed.

The PSCF method (Hopke, 2016; Xin, 2016) was used to identify the possible source areas by analyzing trajectory pathways. HYSPLIT model, developed by the Air Resources Laboratory (ARL) of the United States National Oceanic and Atmospheric Administration (NOAA) (Stein et al., 2016), was used to calculate the 72-h backward trajectories using National Centers for Environmental Prediction (NCEP) reanalysis data. The altitude of the receptor site was set in the height of 500 m above ground level in this study. The entire geographic region covered by the trajectories was divided into an array of grids (defined by the cell indices i and j). The PSCF value of each grid cell was calculated using the following equation:

$$\mathrm{PSCF}_{i,j} = \frac{S_{i,j}}{T_{i,j}} \quad (3)$$

where $S_{i,j}$ represents the number of trajectory endpoints for which the measured pollutant concentration exceeds a threshold value selected for it in the (i, j) grid cell, and $T_{i,j}$ represents the total number of trajectory endpoints that fall in the grid cell.

High PSCF values represent likely source locations. The threshold criterion value was set at 75 $\mu g\,m^{-3}$. To eliminate the uncertainty due to the small values of Tij, an arbitrary weight function Wij was multiplied by the PSCF value, as suggested by Cheng et al. (1993):

$$\mathrm{Wi,j} = \begin{cases} 1.00 & 40 < Ti,j \\ 0.70 & 10 < Ti,j \le 40 \\ 0.42 & 5 < Ti,j \le 10 \\ 0.17 & Ti,j \le 5 \end{cases} \quad (4)$$

3. Results and discussion

3.1. PMRR in NCP and YRD

Table 1 shows the number of $PM_{2.5}$ mass concentration growth processes, average PMRR and average duration time of BJ and SH during the study period of 2013–2016. BJ and SH had 173 and 76 growth processes respectively. The number of $PM_{2.5}$ mass concentration growth processes in BJ was much larger than that in SH. The results indicated the two cities had similar PMRR and duration time. The 4-year average PMRR in BJ and SH was 7.07 ± 8.42 $\mu g\,m^{-3}\,h^{-1}$ in BJ and 6.60 ± 5.99 $\mu g\,m^{-3}\,h^{-1}$ in SH, respectively. The 4-year average duration time in BJ and SH was also similar, with 43.34 ± 23.77 h in BJ and $= 38.51 \pm 21.34$ h in SH. Similar PMRR values were also found between BJ and SH for $PM_{2.5}$ mass concentration growth processes with different duration time (shown in Table S1 in the Supplemental Materials).

The growth processes of BJ mainly occurred in the winter, accounting for about 35% of the total growth processes, followed by 24% in autumn and 24% spring. In SH, $PM_{2.5}$ mass concentration growth processes mainly occurred in winter, accounting for about 55%. Number of $PM_{2.5}$ mass concentration growth processes was the least in summer in both BJ and SH, accounting for 17% and 7% respectively. The seasonal difference of the growth processes was mainly due to the seasonal variations in emissions and meteorological conditions. Residential emissions of coal and biomass burning for house heating in winter were significantly high and contributed largely to high $PM_{2.5}$ pollution (Liu et al., 2016b; Shi

Table 1
The number of $PM_{2.5}$ mass concentrations growth process, average PMRR and average duration for BJ and SH between 18 January 2013 and 31 December 2016.

City	Number					Average PMRR ($\mu g m^{-3} h^{-1}$)	Average duration time (T)
	Total	Spring	Summer	Fall	Winter		
Beijing (BJ)	173	41	29	42	61	7.07 ± 8.42	43.34 ± 23.77
Shanghai (SH)	76	14	5	15	42	6.60 ± 5.99	38.51 ± 21.34

et al., 2017; Sun et al., 2013). In addition, ventilation conditions were poorer in winter than in summer due to slower wind and shallower mixing layer height (Liu et al., 2013; Shu et al., 2017; Yang et al., 2015; Zhang et al., 2014b).

Fig. S3 displays the relative occurrence frequency of PMRR in BJ and SH. PMRR was categorized into seven different intervals ($0 < PMRR < 2$, $2 < PMRR < 4$, $4 < PMRR < 6$, $6 < PMRR < 8$, $8 < PMRR < 10$, $10 < PMRR < 20$, $PMRR > 20$; PMRR in units of $\mu g\ m^{-3}\ h^{-1}$). The results suggest that the PMRR values in BJ and SH were mainly in the range of $2 < PMRR < 8$, accounting for 78% and 74%, respectively. PMRR in BJ had the highest frequency in the interval of $4 < PMRR < 6$, which accounted for 38% and PMRR in SH had the highest frequency in the interval of $2 < PMRR < 4$, which accounted for 32%.

Fig. 1 shows the variation in the number of the growth processes in BJ and SH from 2013 to 2016. A decreasing trend was found for the $PM_{2.5}$ mass concentration growth processes in BJ and SH. On average, the number of $PM_{2.5}$ mass concentration growth processes decreased by 27.45% in BJ and 45.45% in SH from 2013 to 2016. Comprehensive pollution control strategies have been implemented since 2013 in China, such as the Action Plan for Air Pollution Prevention and Control (2013) (Liang et al., 2017; Qiu, 2014). Emissions of major pollutants have declined and resulted in decrease of annual average $PM_{2.5}$ concentrations since 2013 in the NCP and YRD regions (Wang et al., 2017b). The annual average concentration of $PM_{2.5}$ generally decreased by $1.5\ \mu g\ m^{-3}\ year^{-1}$ from 2000 to 2015 under the implementation of 16 phases' air pollution control measures in Beijing (Lang et al., 2017). The declining number of $PM_{2.5}$ mass concentration growth processes confirmed that the pollution control strategies in China have been effective in recent years.

Fig. 2 shows the diurnal variation of the mean (25% and 75% percentiles are also shown in the figure) PMRR in BJ and SH averaged over the respective 173 and 76 growth processes. A three-peak mode diurnal variation of the growth processes was identified in both BJ and SH. The hours with higher PMRR in BJ were around midnight, early morning (hours 8–10) and early evening (hours 18–19). The hours in SH with higher PMRR was similar but 1–2 h earlier in the morning and 1–2 h later in the evening growth processes, compared to those in BJ. A few studies have identified a similar mid-night peak in black carbon and particle number concentrations in Beijing (Hua et al., 2016; Westerdahl et al., 2009),

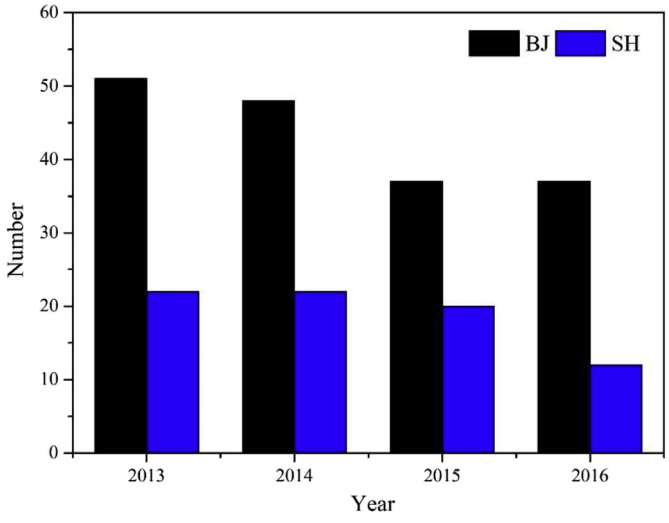

Fig. 1. The number of $PM_{2.5}$ mass concentration growth process in BJ and SH from 2013 to 2016.

because transportation of goods to Beijing via heavy-duty diesel vehicles has been permitted at midnight only, and the number of trucks is large. The first peak might be related to mid-night diesel vehicle emissions, although the contribution to the total $PM_{2.5}$ mass need to be further quantified. The second and third peak might be resulted from vehicles emissions during rush hours and/or cooking activities for breakfast and dinner. Studies indicated that the haze events occurred at 08:00 in North China account for nearly half of total events from 1960 to 2012 (Chen and Wang, 2015; Hua et al., 2016).

3.2. Chemical composition analysis

Wang et al. (2014a, c) suggested that the internal cause of the January 2013 heavy haze pollution episode over central and eastern China was the quick secondary transformation of primary gaseous pollutants to secondary aerosols. Chemical composition analysis revealed that the mass ratio of the sum of secondary inorganic aerosols ($SIA = SO_4^{2-} + NO_3^- + NH_4^+$) to $PM_{2.5}$ increased rapidly during the polluted days in January 2013 at three sites (BJ, SH, and Huaniao) (Wang et al., 2015b). PMRR of the major components (OA, SO_4^{2-}, NO_3^- and NH_4^+) were calculated for the 22 $PM_{2.5}$ mass concentration growth processes in BJ and 19 $PM_{2.5}$ mass concentration growth processes in SH with available composition measurement data. Fig. 3 shows that the PMRR of the four chemical components and the $PM_{2.5}$ total mass during every growth process in BJ and SH. The composition measurements made in BJ are of PM_1. A ratio of 0.7 (i.e., $PM_1 = 0.7{*}PM_{2.5}$) (Wang et al., 2014b), was used to roughly estimated the PMRR of PM_1 mass in BJ. The difference between the PMRR of the total mass and the sum of PMRR of the four components was small in SH, indicating that the four components dominate the total mass of $PM_{2.5}$ in SH. This also held true for most growth processes in BJ. SO_4^{2-}, NO_3^- and NH_4^+ and OA were dominant in the most of $PM_{2.5}$ growth processes of BJ and SH, while other components could also contribute significantly to the $PM_{2.5}$ growths in a few processes in BJ, such as the growth processes on 2013/2/14 and 2013/5/12. During these processes, other components contributed largely to PM total mass growth.

The results also show that different growth processes were contributed by different components. For examples, in BJ OA had the largest PMRR on the growth process on 2013/1/22, while PMRR of SO_4^{2-} on 2013/5/16 and PMRR of NO_3^- on 2013/4/19 was the largest of the four components. The similar phenomenon that different components dominate different growth processes was also found in SH. On average of all the growth processes with available component measurements, the average PMRR of PM_1 (OA, SO_4^{2-}, NO_3^-, and NH_4^+) in BJ was 1.90, 0.95, 0.82 and $0.53\ \mu g\ m^{-3}\ h^{-1}$, respectively. The average PMRR of $PM_{2.5}$ (OA, SO_4^{2-}, NO_3^-, and NH_4^+) in SH was 1.70, 1.18, 1.99 and $1.14\ \mu g\ m^{-3}\ h^{-1}$, respectively. Therefore, OA was more important for the mass concentration growth processes of $PM_{2.5}$ in BJ, while nitrate was more important in SH during the studying periods.

The relative importance of different components in different $PM_{2.5}$ mass concentration growth processes was further confirmed in Fig. 4, which shows the MR values of the three components (i.e., OA, SO_4^{2-} and NO_3^-) during each growth process. Based on the MR values, relative importance of different components to the $PM_{2.5}$ total mass growth during the 41 $PM_{2.5}$ mass concentration growth processes could be identified, and we propose to classify the growth processes in BJ and SH into four general categories:

Category I: The ratios of the three components are all below 1.0, and the ratio of at least one component was around or even under 0.5. In this category, the three major components increased with much slower rates than $PM_{2.5}$ total mass. Therefore, this category belongs to 'other components-dominant growth processes'. The

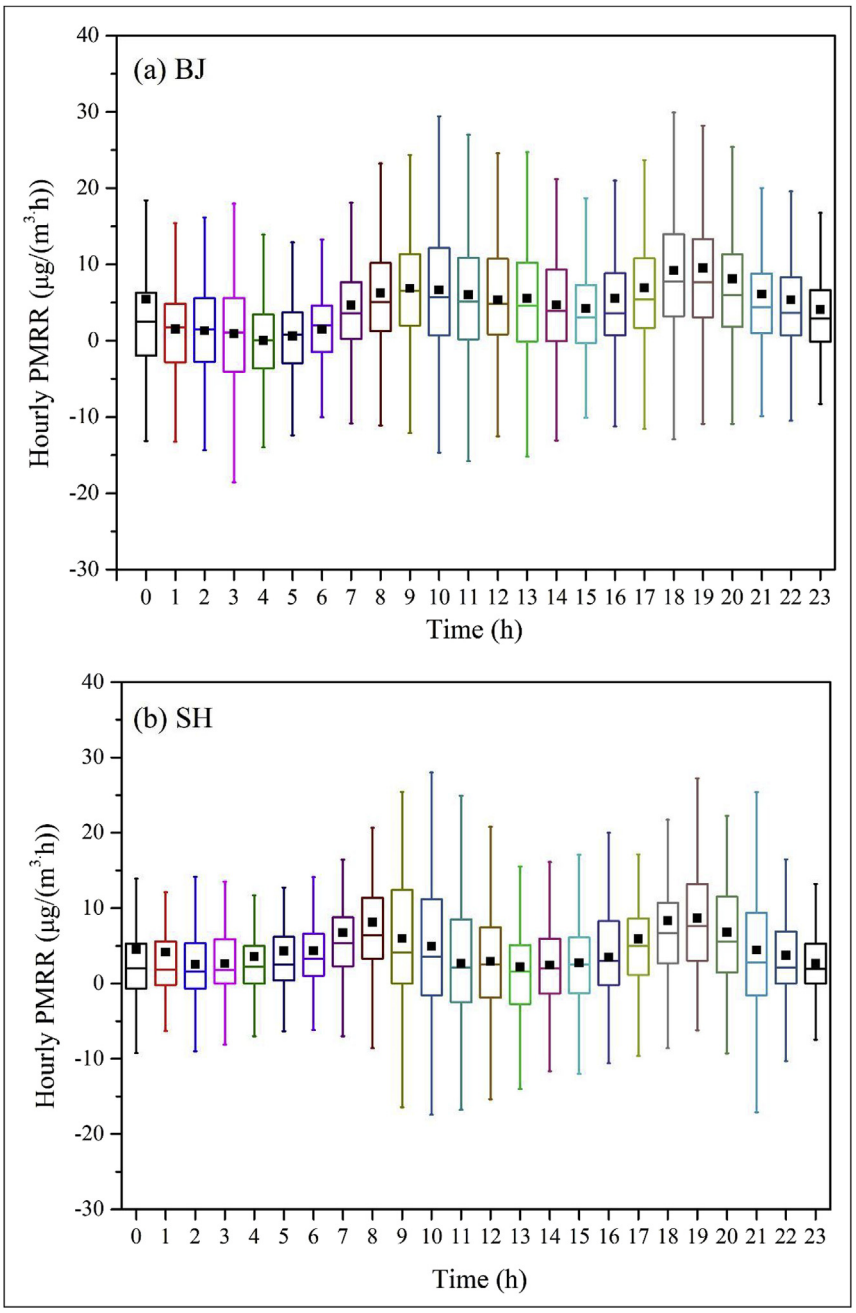

Fig. 2. Diurnal variations of PMRR in BJ (a) and SH (b).

'other components', different from OA, SO_4^{2-} and NO_3^-, were mostly primary components. One of the sources of 'other components' was dust. According to the Sand-Dust Weather Almanac 2013 (http://cyfd.cnki.com.cn/N2016090113.htm) dust events were identified during 2013/02/22, 2013/03/13, and 2013/05/12. But also the other components could come from other sources for other Category I processes, and these sources need to be identified in future studies.

Category II: The ratios of the three components are all in the range of 0.5–1.5, which means the components, including the four components and other components, grew at similar rates as the $PM_{2.5}$ total mass. This category is classified as 'all components-contributing growth processes'. The similar growths in all components could be due to local accumulation with stagnant meteorological conditions, or transport from regions with similar $PM_{2.5}$ compositions.

Category III: The rising ratio of at least one component is above 2.5, which means one or more major components increase with much faster rates than $PM_{2.5}$ total mass. This belongs to the one or more explosive secondary components-dominant growth processes. A few studies (Tan et al., 2018; Wang et al., 2017a, 2018a) have revealed that the atmospheric oxidants in Beijing were high in winter and led to large amount of secondary species formation.

Category IV: Processes that do not fall into any of the above categories are classified as the fourth category, and this category is more like a mixed-factor category. As an example shown in Fig. S4, this category of growth processes typically involved a few different developing stages, and no single factor could explain the entire processes.

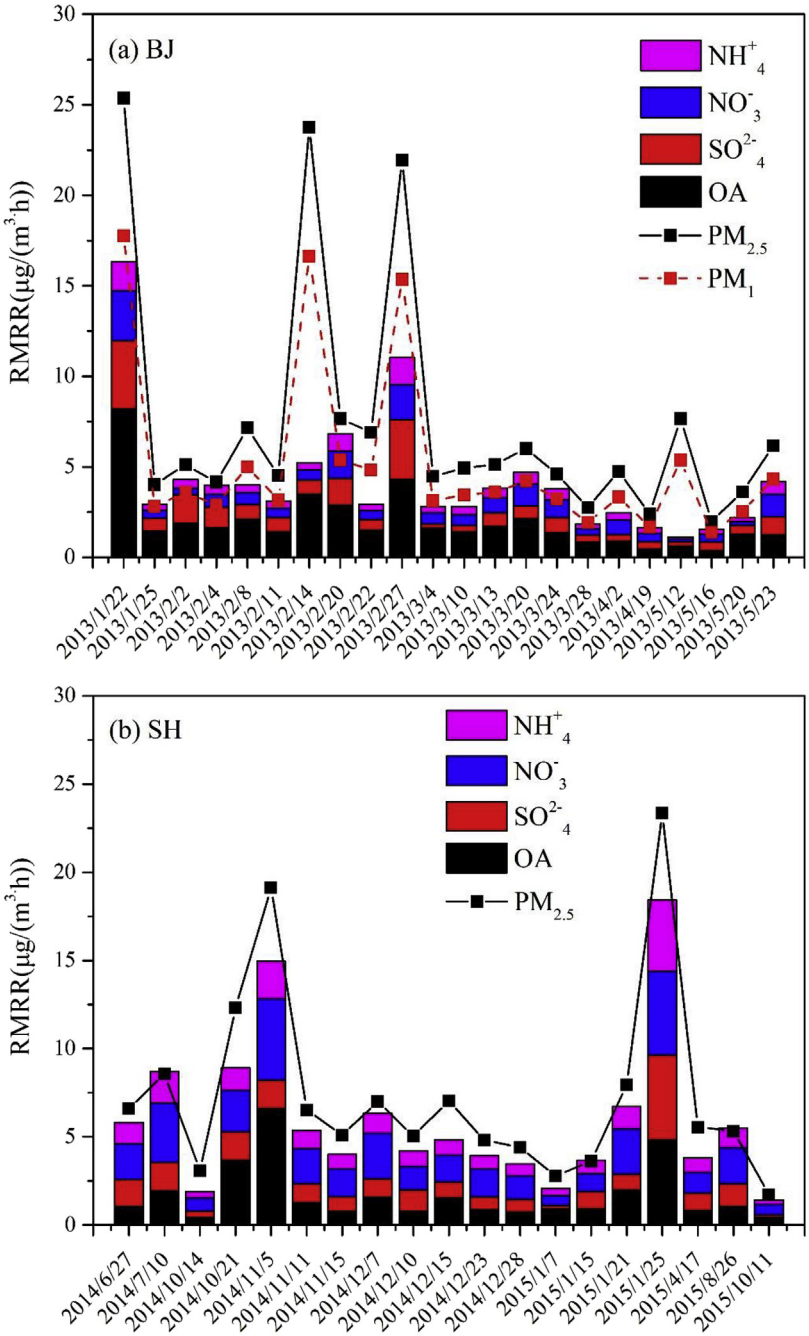

Fig. 3. (a) PMRR of four major components (i.e., OA, SO_4^{2-}, NO_3^- and NH_4^+), $PM_{2.5}$ and PM_1 in BJ, (b) PMRR of four major components and $PM_{2.5}$ in SH.

The $PM_{2.5}$ mass concentration growth processes classified into four categories in BJ and SH were presented in Table S2 in the Supplemental Materials. Out of the 22 growth processes in BJ during January to May 2013, there were 6, 6, 7, and 3 growth processes of Category I-IV, respectively. Out of the 19 growth processes in SH during June 2014 to December 2015, there were 1, 4, 4, and 10 growth processes of Category I-IV, respectively. It should be noted that the findings may be more accurate reflecting the overall causes of $PM_{2.5}$ mass concentration growth processes in SH with continuous data over a full year period but may be less accurate for BJ due to limited data available only in five months in BJ. In addition, comparison of the year 2014 in Shanghai to the year 2013 in Beijing in this study should be cautions as some studies (Zou et al., 2017) showed that the ventilation conditions in January 2013 were extremely poor, which might be linked to Arctic conditions, resulting unprecedentedly high PM concentrations.

3.3. PSCF and meteorological conditions analysis

Regional transport is important for PM pollution in these two regions (Fu et al., 2014, 2016; Hua et al., 2016). In this study, the PSCF method was used to identify the possible source areas of the pollutants reaching BJ and SH in different categories of $PM_{2.5}$ mass concentration growth processes. Fig. 5a-d shows that emissions

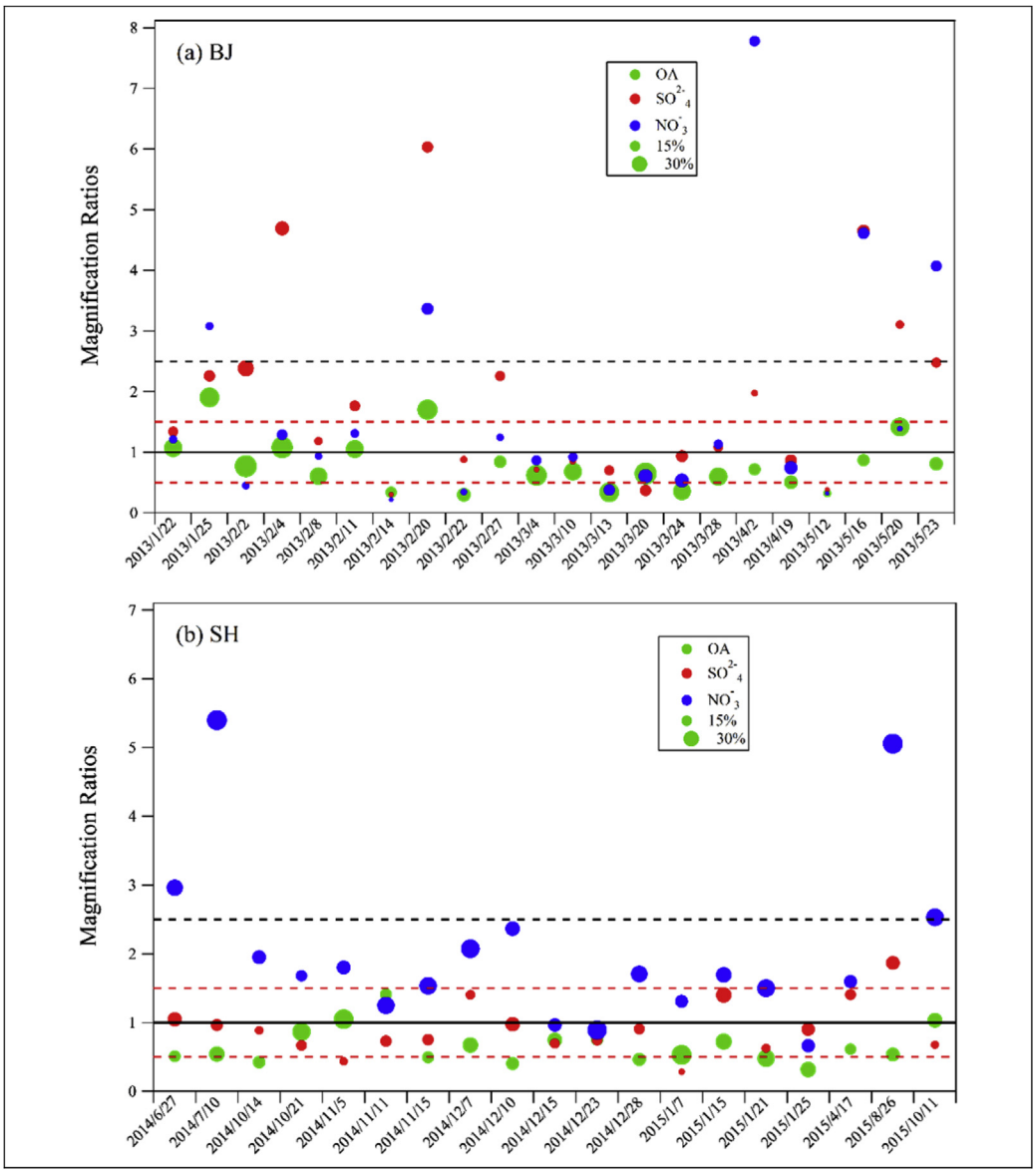

Fig. 4. Classification of the dominant factors of growth processes in BJ (a) and SH (b). The magnification ratios represent the ratios of the magnification of the three components (i.e., OA, SO_4^{2-} and NO_3^-) to that of $PM_{2.5}$ total mass concentrations. The size of the circle represents the concentration proportion of four components to the $PM_{2.5}$ concentrations at the hour of maximum $PM_{2.5}$ concentrations of each growth process.

from heavily polluted areas in the south of Beijing and local emissions had a significant impact on PM concentrations in BJ. From the analysis of Beijing PSCF calculation in category I (Fig. 5a), high PSCF values are found mostly in the south areas to BJ, including large areas in Hebei province, Tianjin, and North path of Shandong province. The results also indicate that BJ is also affected by trajectories far from the northeast and northwest, mainly during the dust events (http://cyfd.cnki.com.cn/N2016090113.htm). Fig. 5b confirmed that local emissions in BJ were responsible for $PM_{2.5}$ accumulations in the 2nd category of $PM_{2.5}$ mass concentration growth processes. Fig. 5c shows that during the explosive secondary components growth processes, the potential sources could come from the south areas to BJ, but also could come from the east/northeast areas to BJ, such as Tangshan. Fig. 5d shows that the potential source areas in category IV were located in the Heibei, Shangdong, and Tianjin. In SH, the potential sources are in SH, Jiangsu and Anhui provinces for most $PM_{2.5}$ mass concentration growth processes, as shown in Fig. 5e-h. During the Category I processes, Fig. 5e, sources were mainly from northwest direction, while for the other three categories, the sources came from more scattered directions.

Clear difference of the source origins for different categories of growth processes was observed in BJ and SH. Long-range transport could have significant contributions in Category I processes in the two cities, which was mainly related to dust events (http://cyfd.cnki.com.cn/N2016090113.htm). In addition, especially in BJ, the regional transport from nearly source areas also had important contribution to Category I processes. While regional transport also played important role in the other three categories of processes, the trajectories was obviously longer in Category I. Compared the trajectories between BJ and SH, source origins for BJ were more concentrated around BJ, while sources for SH were more scattered and distant from SH.

Previous studies indicated that the formation of severe haze

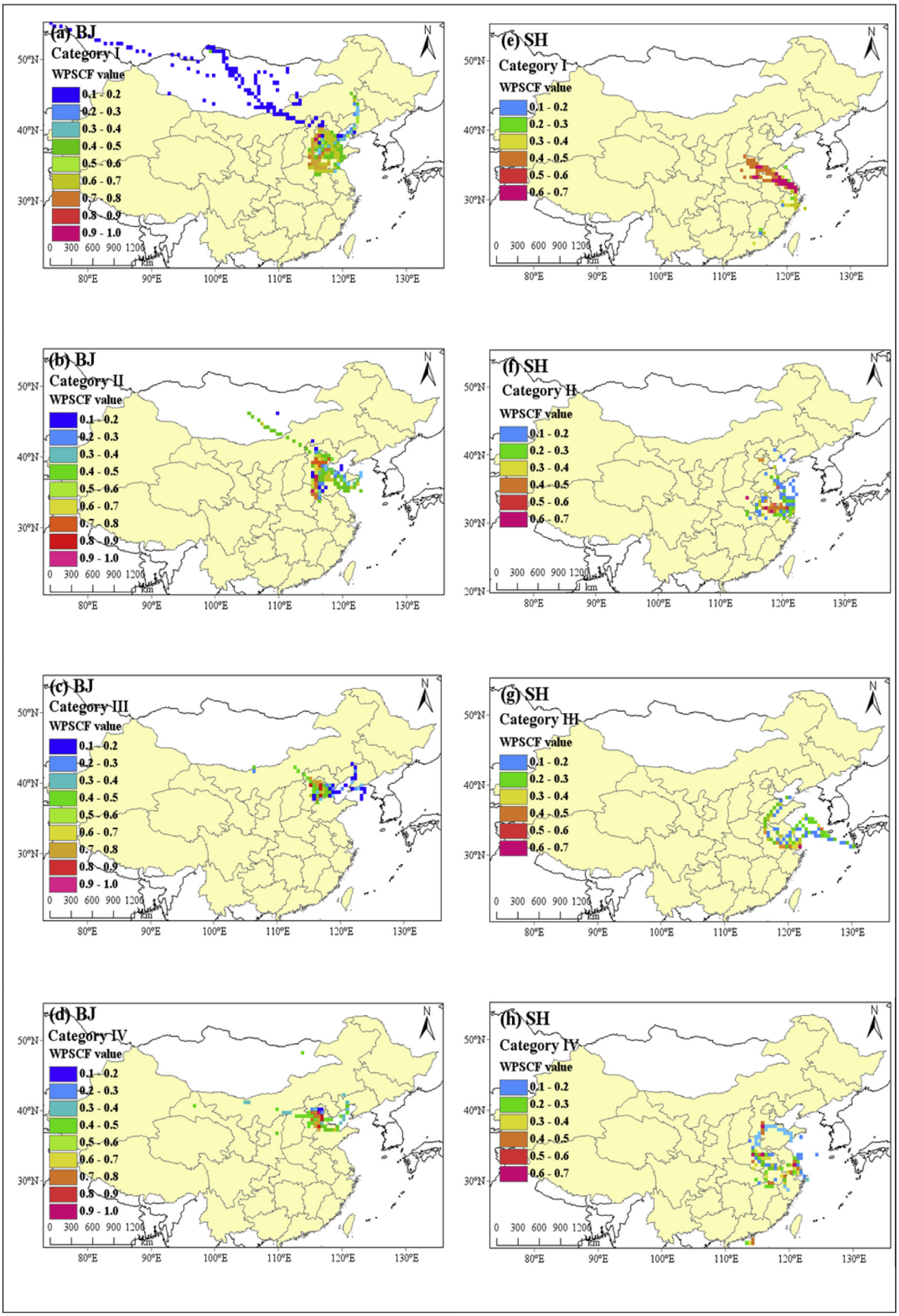

Fig. 5. PSCF plots for the $PM_{2.5}$ mass concentrations growth processes in BJ (a–d) and SH (e–f) by the four general categories.

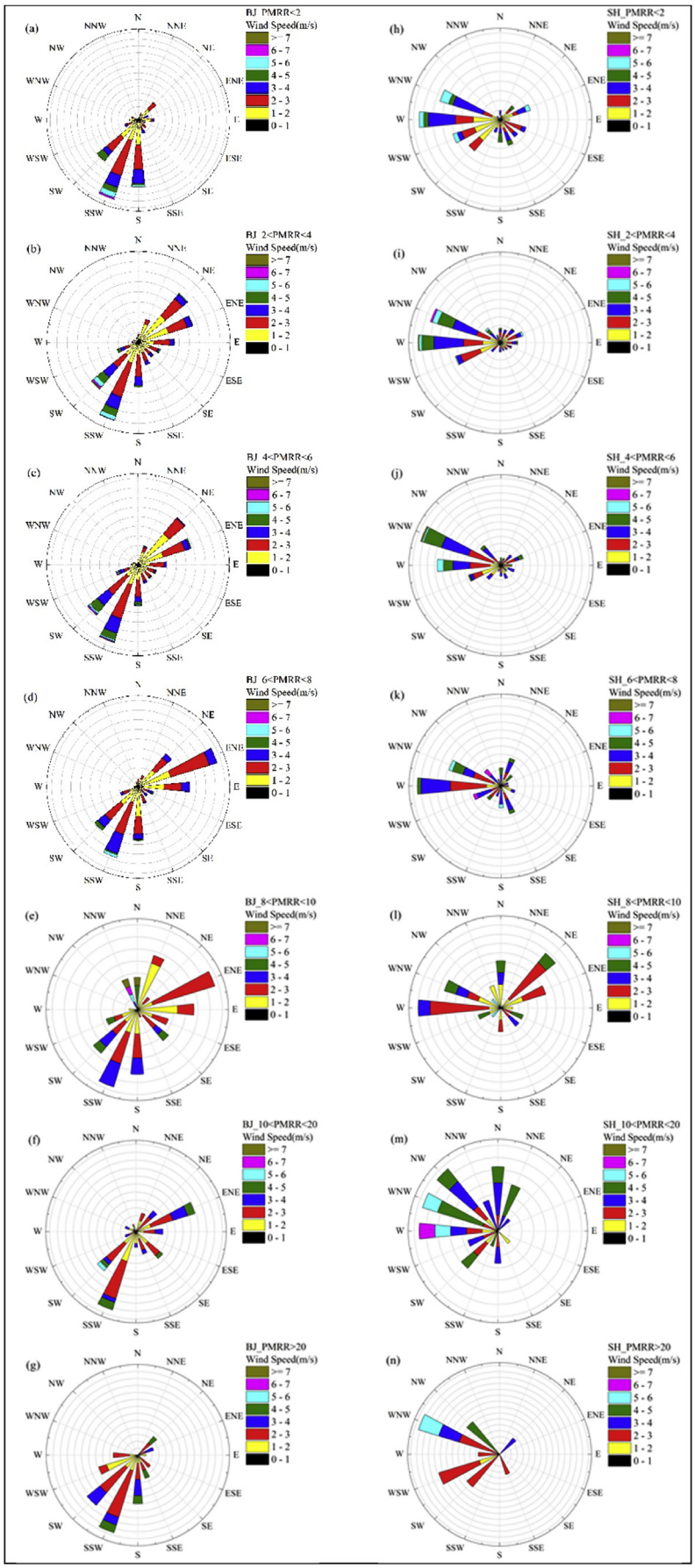

Fig. 6. The wind rose of $PM_{2.5}$ mass concentrations growth processes with low to high PMRR values in BJ (a) and SH (b). The PMRR values were divided into seven different intervals ($0 < PMRR < 2$, $2 < PMRR < 4$, $4 < PMRR < 6$, $6 < PMRR < 8$, $8 < PMRR < 10$, $10 < PMRR < 20$, $PMRR > 20$; PMRR in units of $\mu g\ m^{-3}\ h^{-1}$).

episodes is closely associated with meteorological conditions such as WS, WD, RH and T (Ding and Liu, 2014; Fu and Chen, 2016; Wang et al., 2018b; Yang et al., 2015; Zhang et al., 2014b; Zheng et al., 2015). Meteorological parameters WS, WD, T, and RH were analyzed for all growth processes during the four years in this study. Fig. 6 shows the wind direction and wind speed for growth processes with different PMRR intervals in BJ and SH. As a comparison, the average wind rose for all growth processes and for clean periods ($PM_{2.5} < 75\ \mu g\ m^{-3}$) was shown in Figs. S5 and S6 in the Supplemental Materials, respectively. The results clearly show that specific wind directions affected air pollutants more than other directions. This finding was consistent with a previous study by Zhang et al. (2015). In BJ, the dominant wind directions during growth processes were northeast, south and southwest. This was because easterly and southerly wind could transport pollutants from heavily polluted regions (Wang et al., 2013). While in SH, the dominant wind directions in the growth processes were west to north, indicating that the transport of pollutants from north and west to SH contributed largely to $PM_{2.5}$ mass concentration growth processes (Ying et al., 2014). The four-years average WS of $PM_{2.5}$ mass concentration growth processes in BJ and SH are 1.80 ± 0.97 m/s and 2.35 ± 1.19 m/s, respectively. Previous studies (Lv et al., 2017; Ma et al., 2017; Sun et al., 2016; Zheng et al., 2015) have shown that regional transport could occur with such wind speed in Beijing. Variations of RH and T during the growth processes in BJ and SH are shown in Fig. S7 in the Supplemental Materials.

4. Conclusions

In this study, we analyzed the dynamic accumulation of $PM_{2.5}$ using hourly concentration BJ and SH between 18 January 2013 and 31 December 2016. We focused on the $PM_{2.5}$ mass concentration growth processes from the lowest concentration $<35\ \mu g\ m^{-3}$ to the peak $>150\ \mu g\ m^{-3}$ during 2013–2016. 173 and 76 growth processes were identified in BJ and SH, respectively. The 4-year averaged PMRRs in BJ and SH were $7.11 \pm 9.82\ \mu g\ m^{-3}\ h^{-1}$ and $6.71 \pm 6.89\ \mu g\ m^{-3}\ h^{-1}$, respectively. A decreasing trend was found for the $PM_{2.5}$ mass concentration growth processes in all cities due to emission controls implemented in the past years. Despite the similar PMRR values for $PM_{2.5}$ total mass, the contributions of components were different. Average PMRR of PM_1 OA, SO_4^{2-}, NO_3^-, and NH_4^+ in BJ was 1.90, 0.95, 0.82 and $0.53\ \mu g\ m^{-3}\ h^{-1}$, respectively. Average PMRR of $PM_{2.5}$ OA, SO_4^{2-}, NO_3^-, and NH_4^+ in SH was 1.70, 1.18, 1.99 and $1.14\ \mu g\ m^{-3}\ h^{-1}$, respectively. Therefore, OA was more important for the growth processes of BJ in the first half of 2013, while nitrate was more important in SH during June 2014 to December 2015. To illustrate the importance of different components to the growth processes, we proposed to classify the $PM_{2.5}$ mass concentration growth processes in BJ and SH into four general categories: Category I - 'other components-dominant growth processes', Category II - 'all components-contributing growth processes', Category III - 'one or more explosive secondary components-dominant growth processes', and Category IV - 'mixed-factor growth processes'. In BJ, there were 6, 6, 7, and 3 growth processes of Category I-IV, respectively, during January to May 2013. In SH, there were 1, 4, 4, and 10 growth processes of Category I-IV, respectively, during June 2014 to December 2015. PSFC analysis showed that both long-rang transport and regional transport were important for Category I growth processes. For other categories, regional transport from highly polluted areas was also important for $PM_{2.5}$ growths in BJ and SH. The important source areas were mainly located in Hebei and Shandong for BJ, and Jiangsu and Anhui for SH. The results indicate that even though the PMRR of $PM_{2.5}$ mass concentration growth processes was similar between BJ and SH, the contributing components, the prevailing wind conditions, and the formation processes were substantially different in the two cities. More studies on detailed formation mechanisms of the different $PM_{2.5}$ mass concentration growth processes in the two cities are needed in future.

Acknowledgement

This work was supported by the National Key R&D Program of China (2016YFC0203500, Task #2); the National Natural Science Foundation of China (41675125, 91544221); the Natural Science Foundation of Jiangsu Province under contract no. BK20150904; Jiangsu Distinguished Professor Project 2191071503201; Jiangsu Six Major Talent Peak Project 2015-JNHB-010; and the Priority Academic Program Development of Jiangsu Higher Education Institutions (PAPD).

Appendix A. Supplementary data

Supplementary data to this article can be found online at https://doi.org/10.1016/j.chemosphere.2018.12.200.

References

Bai, X., Shi, P., Liu, Y., 2014. Realizing China's Urban dream. Nature 509, 158–160.
Chang, Y.H., Deng, C.R., Cao, F., Cao, C., Zou, Z., Liu, S.D., Lee, X.H., Li, J., Zhang, G., Zhang, Y.L., 2017. Assessment of carbonaceous aerosols in Shanghai, China - Part 1: long-term evolution, seasonal variations, and meteorological effects. Atmos. Chem. Phys. 17, 9945–9964.
Chang, Y.H., Huang, K., Xie, M.J., Deng, C.R., Zou, Z., Liu, S.D., Zhang, Y.L., 2018. First long-term and near real-time measurement of trace elements in China's urban atmosphere: temporal variability, source apportionment and precipitation effect. Atmos. Chem. Phys. 18, 11793–11812.
Chang, Y.H., Zou, Z., Deng, C.R., Huang, K., Collett, J.L., Lin, J., Zhuang, G.S., 2016. The importance of vehicle emissions as a source of atmospheric ammonia in the megacity of Shanghai. Atmos. Chem. Phys. 16, 3577–3594.
Chen, B., Xiang-De, X.U., 2017. Climatology of wintertime long-distance transport of surface-layer air masses arriving urban Beijing in 2001–2012. Atmos. Environ. 151.
Chen, H., Wang, H., 2015. Haze Days in North China and the associated atmospheric circulations based on daily visibility data from 1960 to 2012. J. Geophys. Res. Atmos. 120, 5895–5909.
Cheng, M.D., Hopke, P.K., Barrie, L., Rippe, A., Olson, M., Landsberger, S., 1993. Qualitative determination of source regions of aerosol in Canadian high arctic. Environ. Sci. Technol. 27, 391–397.
Ding, Y.H., Liu, Y.J., 2014. Analysis of long-term variations of fog and haze in China in recent 50 years and their relations with atmospheric humidity. Sci. China Earth Sci. 57, 36–46.
Fu, H., Chen, J., 2016. Formation, features and controlling strategies of severe haze-fog pollution in China. Sci. Total Environ. 578, 121.
Fu, X., Cheng, Z., Wang, S., Hua, Y., Xing, J., Hao, J., 2016. Local and regional contributions to fine particle pollution in winter of the Yangtze River Delta, China. Aerosol Air Qual. Res. 16, 1067–1080.
Fu, X., Wang, S.X., Cheng, Z., Xing, J., Zhao, B., Wang, J.D., Hao, J.M., 2014. Source, transport and impacts of a heavy dust event in the Yangtze River Delta, China, in 2011. Atmos. Chem. Phys. 14, 1239–1254.
Guo, H., Wang, Y., Zhang, H., 2017. Characterization of criteria air pollutants in Beijing during 2014–2015. Environ. Res. 154, 334–344.
Guo, S., Hu, M., Zamora, M.L., Peng, J., Shang, D., Zheng, J., Du, Z., Wu, Z., Shao, M., Zeng, L., 2014. Elucidating severe urban haze formation in China. Proc. Natl. Acad. Sci. U.S.A. 111, 17373.
Hopke, P.K., 2016. A review of receptor modeling methods for source apportionment. J. Air Waste Manag. Assoc. 66, 237.
Hu, J., Huang, L., Chen, M., Liao, H., Zhang, H., Wang, S., Zhang, Q., Ying, Q., 2017. Premature mortality attributable to particulate matter in China: source contributions and responses to reductions. Environ. Sci. Technol. 51, 9950–9959.
Hu, J., Wang, Y., Ying, Q., Zhang, H., 2014. Spatial and temporal variability of PM2.5 and PM10 over the north China Plain and the Yangtze River Delta, China. Atmos. Environ. 95, 598–609.
Hu, J., Ying, Q., Wang, Y., Zhang, H., 2015a. Characterizing multi-pollutant air pollution in China: comparison of three air quality indices. Environ. Int. 84, 17–25.
Hu, M., Guo, S., Peng, J.F., Wu, Z.J., 2015b. Insight into characteristics and sources of PM_(2.5) in the Beijing–Tianjin–Hebei region, China. Natl. Sci. Rev. 2, 257–258.
Hua, Y., Cheng, Z., Wang, S., Jiang, J., Chen, D., Cai, S., Fu, X., Fu, Q., Chen, C., Xu, B.,

2015. Characteristics and source apportionment of PM 2.5 during a fall heavy haze episode in the Yangtze River Delta of China. Atmos. Environ. 123. S1352231015002708.
Hua, Y., Wang, S., Wang, J., Jiang, J., Zhang, T., Song, Y., Kang, L., Zhou, W., Cai, R., Wu, D., 2016. Investigating the impact of regional transport on PM2.5 formation using vertical observation during APEC 2014 Summit in Beijing. Atmos. Chem. Phys. 16, 15451–15460.
Huang, K., Zhuang, G., Lin, Y., Wang, Q., 2013. How to improve the air quality over mega-cities in China? – pollution characterization and source analysis in Shanghai before, during, and after the 2010 world expo. Atmos. Chem. Phys. 13, 5927–5942.
Huang, K., Zhuang, G., Wang, Q., Fu, J.S., Lin, Y., Liu, T., Han, L., Deng, C., 2014a. Extreme haze pollution in Beijing during January 2013: chemical characteristics, formation mechanism and role of fog processing. Atmos. Chem. Phys. Discuss. 14, 479–486.
Huang, R.J., Zhang, Y., Bozzetti, C., Ho, K.F., Cao, J.J., Han, Y., Daellenbach, K.R., Slowik, J.G., Platt, S.M., Canonaco, F., 2014b. High secondary aerosol contribution to particulate pollution during haze events in China. Nature 514, 218–222.
Ji, D., Li, L., Wang, Y., Zhang, J., Cheng, M., Sun, Y., Liu, Z., Wang, L., Tang, G., Hu, B., 2014. The heaviest particulate air-pollution episodes occurred in northern China in January, 2013: insights gained from observation. Atmos. Environ. 92, 546–556.
Kang, Qiong, Tingting, Jianwei, Zhao, Jingjing, Jiang, Ziqi, Yuanhang, 2014. Chemical characteristics of size-resolved aerosols in winter in Beijing. Environ. Sci. China 26, 1641–1650.
Lang, J., Zhang, Y., Zhou, Y., Cheng, S., Chen, D., Guo, X., Chen, S., Li, X., Xing, X., Wang, H., 2017. Trends of PM2.5 and chemical composition in Beijing, 2000-2015. Aerosol Air Qual. Res. 17, 412–425.
Lelieveld, J., Evans, J.S., Fnais, M., Giannadaki, D., Pozzer, A., 2015. The contribution of outdoor air pollution sources to premature mortality on a global scale. Nature 525, 367–371.
Li, H., Wang, Q.G., Min, S., Wang, J., Cheng, W., Sun, Y., Xin, Q., Wu, H., Meng, Y., Li, F., 2016. Fractionation of airborne particulate-bound elements in haze-fog episode and associated health risks in a megacity of southeast China. Environ. Pollut. 208, 655–662.
Liang, P., Zhu, T., Fang, Y., Li, Y., Han, Y., Wu, Y., Hu, M., Wang, J., 2017. The role of meteorological conditions and pollution control strategies in reducing air pollution in Beijing during APEC 2014 and Victory Parade 2015. Atmos. Chem. Phys. 17, 1–62.
Liu, J., Han, Y., Tang, X., Zhu, J., Zhu, T., 2016a. Estimating adult mortality attributable to PM2.5 exposure in China with assimilated PM2.5 concentrations based on a ground monitoring network. Sci. Total Environ. 568, 1253–1262.
Liu, J., Mauzerall, D.L., Chen, Q., Zhang, Q., Song, Y., Peng, W., Klimont, Z., Qiu, X., Zhang, S., Hu, M., Lin, W., Smith, K.R., Zhu, T., 2016b. Air pollutant emissions from Chinese households: a major and underappreciated ambient pollution source. Proc. Natl. Acad. Sci. U. S. A. 113, 7756–7761.
Liu, X.G., Li, J., Qu, Y., Han, T., Hou, L., Gu, J., Chen, C., Yang, Y., Liu, X., Yang, T., 2013. Formation and evolution mechanism of regional haze: a case study in the megacity Beijing, China. Atmos. Chem. Phys. 13, 4501–4514.
Lv, B., Cai, J., Xu, B., Bai, Y., 2017. Understanding the rising phase of the PM2.5 concentration evolution in large China cities. Sci. Rep. 7, 46456.
Ma, Q., Wu, Y., Zhang, D., Wang, X., Xia, Y., Liu, X., Tian, P., Han, Z., Xia, X., Wang, Y., 2017. Roles of regional transport and heterogeneous reactions in the PM2.5 increase during winter haze episodes in Beijing. Sci. Total Environ. 599–600, 246–253.
Qiu, J., 2014. Fight against smog ramps up. Nature 506, 273.
Quan, J., Liu, Q., Li, X., Gao, Y., Jia, X., Sheng, J., Liu, Y., 2015. Effect of heterogeneous aqueous reactions on the secondary formation of inorganic aerosols during haze events. Atmos. Environ. 122, 306–312.
Shi, Z., Li, J., Huang, L., Wang, P., Wu, L., Ying, Q., Zhang, H., Lu, L., Liu, X., Liao, H., Hu, J., 2017. Source apportionment of fine particulate matter in China in 2013 using a source-oriented chemical transport model. Sci. Total Environ. 601, 1476–1487.
Shu, L., Xie, M., Gao, D., Wang, T., Fang, D., Liu, Q., Huang, A., Peng, L., 2017. Regional severe particle pollution and its association with synoptic weather patterns in the Yangtze River Delta region, China. Atmos. Chem. Phys. 17, 1–31.
Stein, A.F., Draxler, R.R., Rolph, G.D., Stunder, B.J.B., Cohen, M.D., Ngan, F., 2016. NOAA's HYSPLIT atmospheric transport and dispersion modeling system. Bull. Am. Meteorol. Soc. 96, 150504130527006.
Sun, J., Huang, L., Liao, H., Li, J., Hu, J., 2017. Impacts of regional transport on particulate matter pollution in China: a review of methods and results. Curr. Pollut. Rep. 3, 1–10.
Sun, Y., Chen, C., Zhang, Y., Xu, W., Zhou, L., Cheng, X., Zheng, H., Ji, D., Li, J., Tang, X., 2016. Rapid formation and evolution of an extreme haze episode in Northern China during winter 2015. Sci. Rep. 6, 27151.
Sun, Y., Jiang, Q., Wang, Z., Fu, P., Li, J., Yang, T., Yin, Y., 2014. Investigation of the sources and evolution processes of severe haze pollution in Beijing in January 2013. J. Geophys. Res. 119, 4380–4398.
Sun, Y.L., Wang, Z.F., Dong, H.B., Yang, T., Li, J., Pan, X.L., Chen, P., Jayne, J.T., 2012. Characterization of summer organic and inorganic aerosols in Beijing, China with an aerosol chemical speciation monitor. Atmos. Environ. 51, 250–259.
Sun, Y.L., Wang, Z.F., Fu, P.Q., Yang, T., Jiang, Q., Dong, H.B., Li, J., Jia, J.J., 2013. Aerosol composition, sources and processes during wintertime in Beijing, China. Atmos. Chem. Phys. 13, 4577–4592.
Tan, Z., Rohrer, F., Lu, K., Ma, X., Bohn, B., Broch, S., Dong, H., Fuchs, H., Gkatzelis, G.I., Hofzumahaus, A., Holland, F., Li, X., Liu, Y., Liu, Y., Novelli, A., Shao, M., Wang, H., Wu, Y., Zeng, L., Hu, M., Kiendler-Scharr, A., Wahner, A., Zhang, Y., 2018. Wintertime photochemistry in Beijing: observations of ROx radical concentrations in the North China Plain during the BEST-ONE campaign. Atmos. Chem. Phys. 18, 12391–12411.
Tian, M., Wang, H.B., Chen, Y., Yang, F.M., Zhang, X.H., Zou, Q., Zhang, R.Q., Ma, Y.L., He, K.B., 2015. Characteristics of aerosol pollution during heavy haze events in Suzhou, China. Atmos. Chem. Phys. 16, 7357–7371.
Wang, H., Lu, K., Chen, X., Zhu, Q., Chen, Q., Guo, S., Jiang, M., Li, X., Shang, D., Tan, Z., 2017a. High N 2 O 5 Concentrations Observed in Urban Beijing: Implications of a Large Nitrate Formation Pathway, p. 4.
Wang, H., Lu, K., Chen, X., Zhu, Q., Wu, Z., Wu, Y., Sun, K., 2018a. Large particulate nitrate formation from N2O5 uptake in a chemically reactive layer aloft during winter time in Beijing. Atmos. Chem. Phys. 1–27.
Wang, J., Zhao, B., Wang, S., Yang, F., Xing, J., Morawska, L., Ding, A., Kulmala, M., Kerminen, V.M., Kujansuu, J., 2017b. Particulate matter pollution over China and the effects of control policies. Sci. Total Environ. 584–585, 426.
Wang, M., Cao, C., Li, G., Singh, R.P., 2015a. Analysis of a severe prolonged regional haze episode in the Yangtze River Delta, China. Atmos. Environ. 102, 112–121.
Wang, Q., Zhuang, G., Huang, K., Liu, T., Deng, C., Xu, J., Lin, Y., Guo, Z., Chen, Y., Fu, Q., 2015b. Probing the severe haze pollution in three typical regions of China: characteristics, sources and regional impacts. Atmos. Environ. 120, 76–88.
Wang, S., Hao, J., 2012. Air quality management in China:Issues,challenges,and options. J. Environ. Sci. 24, 2–13.
Wang, X., Dickinson, R.E., Su, L., Zhou, C., Wang, K., 2018b. PM 2.5 pollution in China and how it has been exacerbated by terrain and meteorological conditions. Bull. Am. Meteorol. Soc. 99, 105–119.
Wang, Y., Ying, Q., Hu, J., Zhang, H., 2014a. Spatial and temporal variations of six criteria air pollutants in 31 provincial capital cities in China during 2013–2014. Environ. Int. 73, 413–422.
Wang, Y.S., Li, Y., Wang, L.L., Liu, Z.R., Dongsheng, J.I., Tang, G.Q., Zhang, J.K., Yang, S., Bo, H.U., Xin, J.Y., 2014b. Mechanism for the formation of the January 2013 heavy haze pollution episode over central and eastern China. Sci. China Earth Sci. 57, 14–25.
Wang, Z.B., Hu, M., Wu, Z.J., Yue, D.L., 2013. Long-term measurements of particle number size distributions and the relationships with air mass history and source apportionment in the summer of Beijing. Atmos. Chem. Phys. 13, 10159–10170.
Wang, H., Xu, J., Zhang, M., Yang, Y., Shen, X., Wang, Y., Chen, D., Guo, J., 2014c. A study of the meteorological causes of a prolonged and severe haze episode in January 2013 over central-eastern China. Atmos. Environ. 98, 146–157.
Westerdahl, D., Wang, X., Pan, X.C., Zhang, K.M., 2009. Characterization of on-road vehicle emission factors and microenvironmental air quality in Beijing, China. Atmos. Environ. 43, 697–705.
Wu, J., Li, G., Cao, J., Bei, N., Wang, Y., Feng, T., Huang, R., Liu, S., Zhang, Q., Tie, X., 2017. Contributions of trans-boundary transport to summertime air quality in Beijing, China. Atmos. Chem. Phys. 17, 1–46.
Xin, Y., 2016. Identification of long-range transport pathways and potential sources of PM10 in Tibetan plateau uplift area: case study of xining, China in 2014. Aerosol Air Qual. Res. 16, 1044–1054.
Xing, L., Fu, T.M., Cao, J.J., Lee, S.C., 2013. Seasonal and spatial variability of the OM/OC mass ratios and high regional correlation between oxalic acid and zinc in Chinese urban organic aerosols. Atmos. Chem. Phys. 13, 4307–4318.
Xue, W.B., Fei, F.U., Wang, J.N., Tang, G.Q., Yu, L., Yang, J.T., Wang, Y.S., 2014. Numerical study on the characteristics of regional transport of PM_(2.5) in China. China Environ. Sci. 34, 1361–1368.
Yang, Y., Liao, H., Lou, S., 2016. Increase in winter haze over eastern China in recent decades: roles of variations in meteorological parameters and anthropogenic emissions. J. Geophys. Res. Atmos. 121, 13, 050-013,065.
Yang, Y.R., Liu, X.G., Qu, Y., An, J.L., Jiang, R., Zhang, Y.H., Sun, Y.L., Wu, Z.J., Zhang, F., Xu, W.Q., 2015. Characteristics and formation mechanism of continuous extreme hazes in China: a case study in autumn of 2014 in the North China Plain. Atmos. Chem. Phys. Discuss. 15, 10987–11029.
Ying, Q., Wu, L., Zhang, H., 2014. Local and inter-regional contributions to PM 2.5 nitrate and sulfate in China. Atmos. Environ. 94, 582–592.
Yu, X., Shen, L., Xiao, S., Ma, J., Rui, L., Zhu, B., Hu, J., Chen, K., Zhu, J., 2018. Chemical and optical properties of atmospheric aerosols during the polluted periods in a megacity in the Yangtze River Delta, China. Aerosol Air Qual. Res. 19, 103–117.
Zhang, H., Wang, Y., Hu, J., Ying, Q., Hu, X.M., 2015. Relationships between meteorological parameters and criteria air pollutants in three megacities in China. Environ. Res. 140, 242–254.
Zhang, J.K., Sun, Y., Liu, Z.R., Ji, D.S., Hu, B., Liu, Q., Wang, Y.S., 2014a. Characterization of submicron aerosols during a month of serious pollution in Beijing, 2013, Electricity Distribution, 2001. Part 1: Contributions. In: CIRED. 16th International Conference and Exhibition on (IEE Conf. Publ No. 482) v2:50-v52:50.
Zhang, Q., He, K., Huo, H., 2012a. Policy: cleaning China's air. Nature 484, 161–162.
Zhang, R.H., Qiang, L., Zhang, R.N., 2014b. Meteorological conditions for the persistent severe fog and haze event over eastern China in January 2013. Sci. China Earth Sci. 57, 26–35.
Zhang, X.Y., Wang, Y.Q., Niu, T., Zhang, X.C., Gong, S.L., Zhang, Y.M., Sun, J.Y., 2012b. Corrigendum to "Atmospheric aerosol compositions in China: spatial/temporal variability, chemical signature, regional haze distribution and comparisons with global aerosols " published in Atmos. Chem. Phys., 12, 779–799, 2012. Atmos. Chem. Phys. 11, 26571–26615.
Zhang, Y.L., Cao, F., 2015. Fine particulate matter (PM 2.5) in China at a city level. Sci.

Rep. 5, 14884.
Zheng, G., Su, H., Zhang, Q., Cheng, Y., He, K., 2015. Exploring the severe winter haze in Beijing: the impact of synoptic weather, regional transport and heterogeneous reactions. Atmos. Chem. Phys. 15, 2969–2983.
Zou, Y.F., Wang, Y.H., Zhang, Y.Z., Koo, J.H., 2017. Arctic sea ice, Eurasia snow, and extreme winter haze in China. Sci. Adv. 3.